

# Catalytic activity of Cu–Zn–Al–Mn admixed with gamma-alumina for the synthesis of DME from syngas: manganese effect or just method of preparation?

Jelliarko Palgunadi · Indri Yati · Kwang Deog Jung

Received: 12 December 2009 / Accepted: 11 May 2010 / Published online: 4 June 2010  
© Akadémiai Kiadó, Budapest, Hungary 2010

**Abstract** A series of methanol synthesis catalysts, CuO/ZnO/Al<sub>2</sub>O<sub>3</sub> and CuO/ZnO/Al<sub>2</sub>O<sub>3</sub> containing 5 mol% of manganese physically admixed with  $\gamma$ -Al<sub>2</sub>O<sub>3</sub> were tested for the direct synthesis of dimethyl ether from syngas. The catalysts were prepared by coprecipitation of the metal nitrates with several types of alkali carbonate solution. Aqueous solutions of Na<sub>2</sub>CO<sub>3</sub>, NaHCO<sub>3</sub>/Na<sub>2</sub>CO<sub>3</sub> buffer, and NaHCO<sub>3</sub> were used as the precipitating agents to investigate the effects of the preparation method on the microstructure of the precursors and on the physico-chemical properties and reactivity of the resulting catalysts. It was found that the most responsible factor in determining the catalytic activity of the methanol synthesis catalyst is the preparation method rather than the incorporation of manganese as the structure modifier. There is a substantial correlation between the copper metal surface area and the activity of the catalyst derived from the structurally active precursor, hydrotalcite-like layered double hydroxides.

**Keywords** Methanol · Dimethyl ether · Cu–Zn-based catalyst · Syngas · Preparation method

## Introduction

Dimethyl ether (DME) with the formula of (CH<sub>3</sub>)<sub>2</sub>O is an important intermediate for the production of other chemical compounds. Recently, the application of DME as

---

J. Palgunadi (✉)  
Department of Chemistry, Kyung Hee University, 1-Hoegi-dong, Dongdaemoon-gu, Seoul 130-701,  
Republic of Korea  
e-mail: jelliarko@gmail.com

I. Yati · K. D. Jung  
Clean Energy Research Center, Korea Institute of Science and Technology, Seoul 136-791,  
Republic of Korea

an alternative fuel or as a fuel additive for vehicles and domestic cooking gas has received much attention [1]. DME can be synthesized directly from syngas in a single step process which is called as the “syngas-to-dimethyl ether” process. Thermodynamic, technological and economical calculations point out that the direct synthesis process is more favorable than the traditional methanol dehydration process [1, 2]. DME production will be dependent on the activity of the methanol synthesis catalyst because the methanol formation has been believed as the rate limitation step among the series of reactions [3]. To date, Cu–Zn–Al oxides is still considered as the most industrially important type of catalysts for methanol synthesis [2, 4–6]. Later, a methanol synthesis catalyst can be mechanically mixed with a methanol dehydration catalyst (porous solid acids for example,  $\gamma$ -Al<sub>2</sub>O<sub>3</sub> or zeolite) for the direct DME synthesis [7].

The Cu–Zn–Al catalyst is conventionally prepared from aqueous solutions of copper, zinc and aluminum nitrates coprecipitated with a solution of alkali carbonate or bicarbonate to produce a solid catalyst precursor, Cu–Zn–Al-hydroxycarbonates. Heat treatments on the precursor result in the Cu–Zn–Al-oxides. In the chemistry of catalyst preparation via coprecipitation, the formation of a structurally active precursor depends on the preparation conditions such as the type of precipitating agent, pH, coprecipitation temperature, and aging time [8–10]. For example, the structure of the precursor is greatly affected by the rate of addition of the metal nitrates and the concentration of the sodium bicarbonate solution [11]. A structurally active precursor is a precursor possessing special microstructures (i.e. malachite, aurichalcite, or hydrotalcite) that induces the creation of active species during heat treatments. It is worth mentioning that highly dispersed nano-size copper particles, the active species of the methanol synthesis catalyst are readily generated from thermal decompositions of the Cu–Zn–Al-hydrotalcites [8, 9].

Although developments of Cu–Zn–Al-based catalysts have reached a certain maturity, research on this catalytic system is still very active. A microstructure modification by an addition of a fourth component into the Cu–Zn–Al-oxide is expected to improve the catalytic activity and stability [7, 12]. For example, manganese (or other promoters such as gallium, yttrium, and lanthanum) was suggested as a promoter to increase the dispersion and reducibility of copper and therefore it improves the catalytic reactivity. Weide Zhang et al. and Taghizadeh et al. developed a quaternary catalyst of Cu–Zn–Al–Mn and reported the catalytic enhancements for the methanol formation as well as for the DME synthesis [6, 12, 13]. Unfortunately, these works did not reveal and discuss in detail the effect of the preparation method on the formation of the precursors and on the performances of the resulted catalysts. Importantly, the most responsible factor for the high reactivity of the Cu–Zn–Al catalyst is still unclear to us, it may be the presence of manganese or the method of preparation. Our hypothesis is if the earlier factor is the most responsible factor, the catalytic activity is independent or just slightly dependent on the latter one.

To test our hypothesis, series of Cu–Zn–Al and Cu–Zn–Al–Mn as the models of the methanol synthesis catalyst were prepared using various preparation methods. Type of carbonate as the precipitating agent was selected as the variable of the preparation method because the nature of precipitating agent significantly

determines the microstructure of the catalyst precursor. To our knowledge, the effect of various types of alkali carbonate for the preparation of the Cu–Zn–Al-hydroxycarbonates including those containing metallic promoter has never been investigated systematically. The catalysts in conjunction with  $\gamma$ -Al<sub>2</sub>O<sub>3</sub> then were evaluated for the direct synthesis of DME from syngas. Finally, the microstructures of the precursors, the physicochemical properties of the corresponding catalysts, and the catalytic reactivity are correlated.

## Experimental

### Catalyst preparation

The methanol synthesis catalysts, Cu–Zn–Al with the mol% ratios of Cu:Zn:Al = 6:2.5:1.5, and Cu–Zn–Al containing manganese with the mol% ratios of Cu:Zn:Al:Mn = 6:2.5:1:0.5, denoted as CZA and CZAMn, respectively, were prepared by simultaneously coprecipitating their nitrate solutions with an aqueous carbonate solution at pH  $\sim$ 7 under a room temperature condition. Notations of the prepared catalysts and types of the precipitant are listed in Table 1.

In a typical catalyst preparation, Cu(NO<sub>3</sub>)<sub>2</sub>·3H<sub>2</sub>O, Zn(NO<sub>3</sub>)<sub>2</sub>·6H<sub>2</sub>O, Al(NO<sub>3</sub>)<sub>3</sub>·9H<sub>2</sub>O, with/without Mn(NO<sub>3</sub>)<sub>2</sub>·6H<sub>2</sub>O were dissolved in distilled water to get 250 mL of the metal nitrates solution with the total molar concentration of 0.3 M. A stock solution either from the three different precipitating agents was chosen to prepare each of the catalyst precursor. Into a 1000 mL beaker glass initially filled with 200 mL of distilled water, the solution of the metal nitrates and the solution of the precipitating agent were dropped simultaneously within 1.5 h under a vigorous agitation while the pH of the slurry was carefully maintained in a range of 6.90–7.10. Following the completion of the coprecipitation process, the slurry was aged at room temperature by stirring further for 2 h.

The precipitate was filtered, washed with distilled water and stirred for 12 h. This procedure was repeated for six times sufficiently for the slurry to reach pH  $\sim$ 7.0. The cake was dried at room temperature overnight and then was dried in an oven at 110 °C for 24 h. The catalyst precursor was calcined under static air at 350 °C for 3 h with a ramping temperature of 2 °C/min. The oxide catalyst then was ground

**Table 1** Notations of the methanol synthesis catalysts, the formulated mol% ratios of the component, and the types of the precipitating agent

Catalyst	Designated Cu/Zn/Al/Mn mol% ratios	Precipitating agent
CZA–A	60/25/15	1.0 M of Na <sub>2</sub> CO <sub>3</sub>
CZAMn–A	60/25/10/5	
CZA–B	60/25/15	1.0 M of buffer, pH 8.5 consisting of Na <sub>2</sub> CO <sub>3</sub> and NaHCO <sub>3</sub>
CZAMn–C	60/25/15/5	
CZA–C	60/25/15	1.0 M of NaHCO <sub>3</sub>
CZAMn–C	60/25/10/5	

to  $\sim 0.18$  mm and was mixed mechanically with an equivalent amount of the same particle size  $\gamma$ - $\text{Al}_2\text{O}_3$  (methanol dehydration catalyst) for the DME synthesis test.

### Catalyst characterizations

Crystal structures of the samples were analyzed by powder X-ray diffraction (XRD) spectroscopy on a Shimadzu 6000 X-ray diffractometer system (Cu  $K_\alpha$  radiation, 40 kV, 30 mA). Reducibility was measured by temperature programmed reduction ( $\text{H}_2$ -TPR) experiment using an apparatus setting found in the literature elsewhere [14]. In a typical  $\text{H}_2$ -TPR experiment, a catalyst sample of about 30 mg was heated up to 450 °C at a heating rate of 10 °C/min under a flow of 5 vol.%  $\text{H}_2$  in Ar (10 mL/min) and was dwelt at this temperature for 30 min.  $\text{Cu}_2\text{O}$  was used as the standard calibration for calculating the  $\text{H}_2$  consumption. The copper surface area ( $S_{\text{Cu}}$ ) was determined by  $\text{N}_2\text{O}$  titration using a pulse flow experiment following the literature [15] using a Porapak N column for the separation of  $\text{N}_2\text{O}$  and  $\text{N}_2$ . In a typical experiment, about 50 mg of a sample was loaded into a tubular glass reactor and was reduced using 5 vol.%  $\text{H}_2$  in Ar stream at 250 °C for 1 h. After the reduction step, the reactor was purged with a He flow at 250 °C for 30 min and was cooled down to 90 °C at which the  $\text{N}_2\text{O}$  titrations were carried out. A surface copper density of  $1.47 \times 10^{19}$  atoms/ $\text{m}^2$  and the adsorption stoichiometry of  $\text{Cu}:\text{O} = 2:1$  (based on the equation:  $2\text{Cu} + \text{N}_2\text{O} \rightarrow \text{Cu}-\text{O}-\text{Cu} + \text{N}_2$ ) were taken into consideration. The elemental composition of the samples was determined by energy dispersion scanning (EDS) analysis using a Hitachi FE-SEM S-400 microscope at an accelerating voltage of 0.5–30 kV.

### Activity tests

The activity test for the DME synthesis was carried out in a fix bed tubular reactor (i.d.: 1/8", length: 30 cm) loaded with 1.0 g of an admixed catalyst. Prior to the catalytic activity measurement, the catalyst mixture was reduced in a stream of 5%  $\text{H}_2/\text{N}_2$  balance with a sequential step as follows: 1st step: treatment at 100 °C/0.5 h, 2nd step: reduction at 180 °C/0.5 h, 3rd step: reduction at 240 °C/2 h, 4th step: reduction at 280 °C/0.5 h. The catalytic reaction was conducted under the following conditions:  $\text{H}_2:\text{CO} = 1.5$ , GHSV of 6000, pressure of 600 psig ( $\sim 4.13$  MPa), and the temperature from 240 to 270 °C. The feed gases were purified through a mixture of molecular sieve and activated carbon prior to entering the reaction vessel. The effluent gas mixture was analyzed using an on-line gas chromatography equipped with a Porapak Q column and a thermal conductivity detector.

## Results and discussion

### Catalysts preparation

In our experiments, the precursors of Cu–Zn–Al and Cu–Zn–Al–Mn were obtained from the metal nitrate solutions coprecipitated by a solution of sodium carbonate,

sodium bicarbonate or their mixture. It was relatively easy to control the rate of coprecipitation and to adjust the pH to 7.0 using the  $\text{NaHCO}_3$  solution because it has an amphoteric property. A buffer solution made from alkali carbonate/bicarbonate was also beneficial for the coprecipitation since it has a buffer capacity to maintain the necessary pH. The precipitation process at pH 7.0 was selected because this pH level was mentioned as the suitable condition for the formation of the hydrotalcite-like structure [10].

The precipitate was thoroughly washed in distilled water under stirring for 12 h. This procedure was repeated six times to eliminate the nitrate ions and sodium content. In the course of the consecutive washing and long agitation time, where an aging process might take place, the slurries of all CZA precursors underwent a visible color transition from blue to greenish blue regardless the type of the precipitant. Moreover, the physical appearance of the slurries also obviously changed from a powder-like to a gel-like material which can be associated with a phase transition. These phenomena indicate that all CZA precursors experienced an aging process during washing and agitation and altered their physicochemical properties. CZA–B and CZA–C hydroxycarbonates were found to have a relatively fast color transition suggesting that the precipitant containing  $\text{NaHCO}_3$  is advantageous to drive the phase transition of the CZA precursor. Previous work described a structure modification of Cu–Zn-based catalyst precursor after the aging process [16]. Accordingly, a CuO/ZnO catalyst derived from a precursor with a color transition is much more active compared to that obtained from a precursor without a color transition.

Interestingly, neither a color transition nor a gel-like formation could be observed from CZAMn–B and CZAMn–C hydroxycarbonates. Meanwhile, the color transition of CZAMn–A precursor (coprecipitated using  $\text{Na}_2\text{CO}_3$ ) was not profound although it still exhibited a gel-like structure. It can be inferred that the preparation of Cu–Zn–Al–Mn by the coprecipitation technique is highly sensitive to the type of the precipitating agent.

#### Characterization of the catalysts (XRD, EDS, and TPR)

The XRD patterns of the CZA and CZAMn precursors, dried in an oven at 110 °C, are displayed in Figs. 1 and 2, respectively. Liu et al. reported that a hydroxycarbonates of Cu–Zn binary system with a molar ratio of  $\text{Cu}/\text{Zn} = 2/1$  under a long aging process underwent a color transition which was suggested as the indication of some phase transition from copper nitrate hydroxide  $\text{Cu}_2(\text{NO}_3)(\text{OH})_2$ , georgeite, and hydrozincite,  $\text{Zn}_5(\text{CO}_3)_2(\text{OH})_6$  to other phases such as rosasite (or zincian malachite)  $(\text{Cu},\text{Zn})_2\text{CO}_3(\text{OH})_2$ , and auricalchite,  $(\text{Zn},\text{Cu})_5(\text{CO}_3)_2(\text{OH})_6$  [16]. The latter two phases likely alter into a CuO–ZnO solid-solution after heat treatments. The CuO highly dispersed in the ZnO matrix is said to work synergistically and is responsible for the sharp increase of the catalytic activity [15].

Even though all CZA precursors in our experiment exhibited the color shift, the presence of the rosasite or auricalchite phase can hardly be seen from the XRD patterns. Indeed, the characteristic peaks corresponding to the hydrotalcite-like (HTlc) structure with the stoichiometric formula of  $\text{Cu}_x\text{Zn}_{6-x}\text{Al}_2(\text{OH})_{16}(\text{CO}_3)_4 \cdot 4\text{H}_2\text{O}$

**Fig. 1** XRD patterns of oven-dried CZA precursors showing (triangle) hydrotalcite, (filled triangle) malachite, (circle)  $\text{Cu}_2\text{CO}_3(\text{OH})_2$ , and (filled circle) CuO phases: (a) CZA-A, (b) CZA-B, and (c) CZA-C

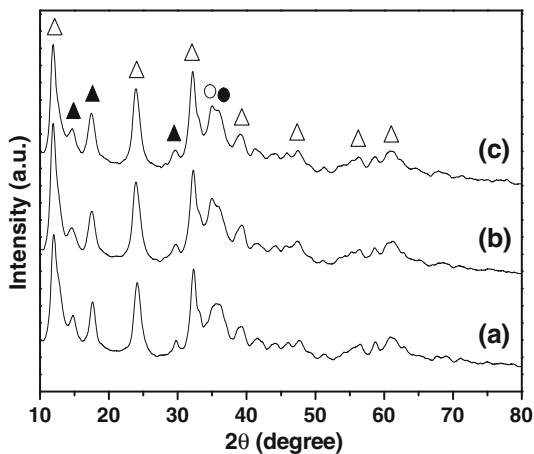
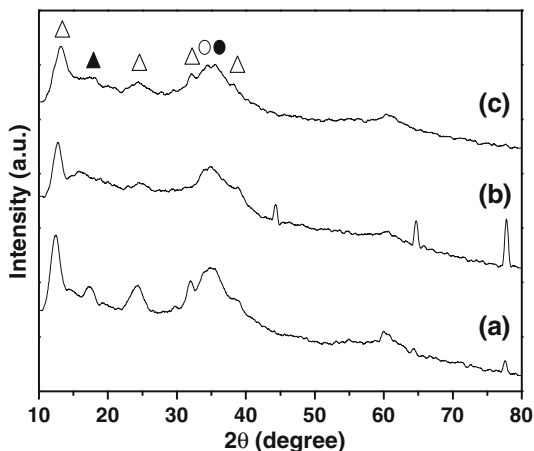


**Fig. 2** XRD patterns of oven-dried CZAMn precursors showing (triangle) hydrotalcite, (filled triangle) malachite, (circle)  $\text{Cu}_2\text{CO}_3(\text{OH})_2$ , and (filled circle) CuO phases: (a) CZAMn-A, (b) CZAMn-B, and (c) CZAMn-C



and malachite are dominant. These circumstances might be explained by the facts that the malachite, aurichalcite, and rosasite structures are primarily formed in the Cu–Zn-system, while the HTlc is generated when aluminum is added [17]. The similar structure found in all CZA precursors suggests that the nature of the precipitants used in this study does not greatly affect the bulk structure of the precursors.

A previous work suggested that the HTlc phase co-exists with the malachite phase when the atomic ratio of copper,  $r = \text{Cu}/(\text{Cu} + \text{Zn})$  is in the range of 0.5–0.9 [8]. As can be seen in Table 2, the atomic ratios of Cu to (Cu + Zn) for all samples are close to 0.70. Other phases, CuO and  $\text{Cu}_2\text{CO}_3(\text{OH})_2$  also appear which can be ascribed to the deviant behavior of  $\text{Cu}^{2+}$  when the ratio of  $\text{Cu}^{2+}/\text{Zn}^{2+}$  is higher than 1. The presence of CuO along with HTlc is also quite possible due to the Jahn-Teller effect [18].

On the contrary, the XRD spectra of all prepared CZAMn precursors clearly show a collapsed HTlc-like structure even with the incorporation of a very low

**Table 2** Physicochemical properties of the fresh calcined CZA and CZAMn series

Catalyst	EDS results		H <sub>2</sub> -TPR results		N <sub>2</sub> O titration results		
	Actual mol% ratio	Cu/(Cu + Zn) ratio	T <sub>max</sub> / °C	H <sub>2</sub> uptake/ mmol g <sup>-1</sup>	S <sub>Cu</sub> / m <sup>2</sup> g <sup>-1</sup>	t <sub>Cu</sub> /nm	D <sub>Cu</sub> (%)
CZA–A	55/19/26	0.74	278	8.8	13.5	50	3.7
CZAMn–A	62/19/16/2	0.77	282	9.2	13.0	52	3.4
CZA–B	64/21/15	0.75	276	9.0	16.1	42	4.4
CZAMn–B	55/22/20/3	0.71	289	8.1	9.6	70	2.9
CZA–C	58/20/22	0.74	284	8.8	16.2	42	4.5
CZAMn–C	64/19/15/2	0.77	288	8.1	9.6	70	2.9

manganese concentration implying that the addition of manganese distracts the formation of the HTlc-like structure. CZAMn–B and CZAMn–C hydroxycarbonates exhibit poor HTlc structure and only CZAMn–A hydroxycarbonates relatively retains that structure. This collapsed structure is also probably the reason for the hardly-observable color transition in all CZAMn precursors.

The XRD patterns of the calcined CZA and CZAMn are displayed in Figs. 3 and 4, respectively. Calcination under air at 350 °C for 3 h with a ramping temperature of 2 °C/min was applied and was considered to sufficiently decompose all hydroxycarbonates to the corresponding metal oxides. Calcination temperatures higher than 350 °C might lead the copper particles to partly sinter and a faster heating rate will produce bigger CuO crystals [19]. As shown in Fig. 3, all calcined CZA catalysts show similarly strong peak intensities of CuO phase (tenorite) and some weak reflections of ZnO phase (zincite). Those peaks are not finely resolved probably due to the high copper content. The broad reflections of CuO and ZnO might also indicate that copper partially dissolved in Zn matrix or CuO is in intimate contact with ZnO phase [17]. Aluminum in all CZA catalysts is assumed to present as an amorphous alumina [20].

**Fig. 3** XRD patterns of CZA catalysts after calcination at 350 °C showing (*inverted filled triangle*) CuO and (*inverted open triangle*) ZnO phases: (a) CZA–A, (b) CZA–B, and (c) CZA–C

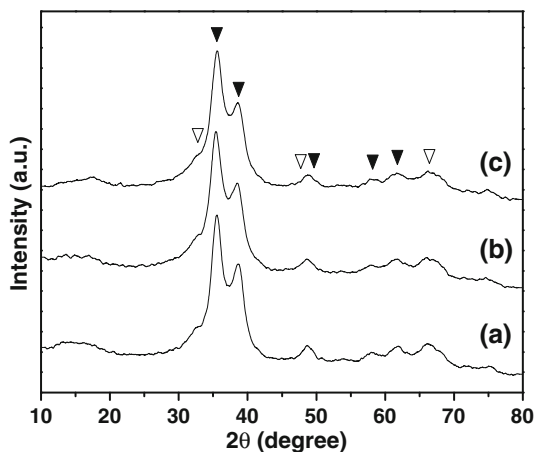
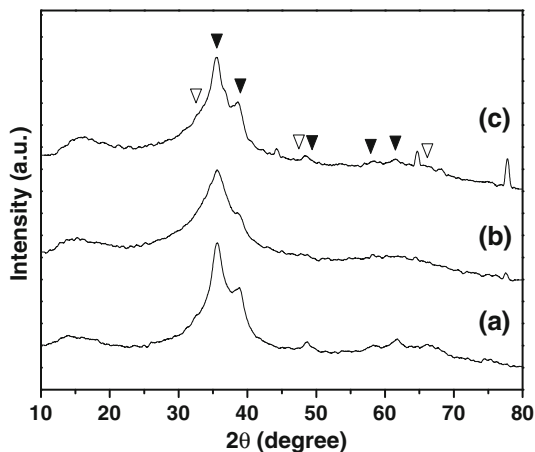


**Fig. 4** XRD patterns of CZAMn catalysts after calcination at 350 °C showing (inverted filled triangle) CuO and (inverted open triangle) ZnO phases: (a) CZAMn-A, (b) CZAMn-B, and (c) CZAMn-C



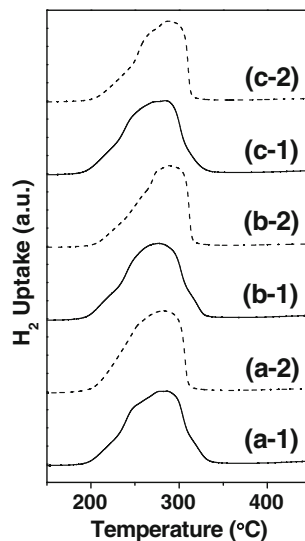
The XRD patterns of the calcined CZAMn samples exhibit low peak intensities of CuO phase and some very weak reflections of ZnO phase which can also be associated to the formation of CuO–ZnO solid solution and a uniform distribution of CuO particles in the ZnO phase. However, two distinctive peaks at  $\sim 64^\circ$  and  $77^\circ$  and a minor one at  $\sim 44^\circ$  probably correlated to a Zn–Al oxide phase appear on the XRD pattern of the CZAMn–B precursor and the CZAMn–C catalyst. The explanation of that phase formation is still unknown to us but it strongly suggests that the precipitant containing  $\text{NaHCO}_3$  is not compatible for the Cu–Zn–Al–Mn preparation. The poor formation of HTlc structure in those CZAMn precursors could be the reason for the presence of the unexpected phase.

The actual bulk chemical compositions of the calcined catalysts analyzed using an energy dispersion scanning (EDS) analysis (Table 2) were found to be somewhat different from the designated mol ratios. These discrepancies are possibly due to the incomplete precipitation of the metal ions under the applied pH condition (about 7.0) or because of the purity of the starting materials. For example, the highly hygroscopic nature of all metal nitrates for the catalyst preparation might affect the actual amount required. The low manganese contents ( $<5$  mol%) found in all CZAMn samples might be associated with manganese leaching during washing steps. In general, the catalytic activity is not immediately correlated with the bulk copper concentration.

The amount of hydrogen uptakes from the TPR analysis of the fresh catalysts are listed in Table 2 and the TPR profiles are displayed in Fig. 5. It is not surprising that broad TPR peaks were observed in all prepared catalysts recalling that the high copper concentration ( $\sim 60$  mol%) accounts for the overlapped reducibility of dispersed CuO and bulk CuO [21]. All the copper species in the Cu–Zn–Al-oxides can be reduced depending on the applied temperature of reduction.  $\text{Cu}^{2+}$  from the amorphous CuO dispersed on the catalyst surface is suggested to reduce to copper at a lower temperature. Subsequently, reduction steps of  $\text{Cu}^{2+}$  to  $\text{Cu}^+$  and last to  $\text{Cu}^0$  take place in the CuO–ZnO alloy or in the bulk CuO at a higher temperature [16, 22, 23]. As shown in Fig. 5, the  $\text{H}_2$ -TPR profiles over the CZA catalysts consist of a wide shoulder



**Fig. 5** TPR profiles of CZA and CZAMn catalysts: (a-1) CZA–A, (a-2) CZAMn–A, (b-1) CZA–B, (b-2) CZAMn–B, (c-1) CZA–C, and (c-2) CZAMn–C



at the beginning, a broad peak with single maximum, and a small shoulder at the end associated with the low temperature reduction of the amorphous CuO to Cu<sup>0</sup>, the reduction of the CuO–ZnO solid solution, and the reduction of the bulk CuO, respectively. Differently, the TPR profiles over the CZAMn catalysts only showed a minute shoulder and a broad peak attributed to the reduction of a small amount of the amorphous CuO and the major reduction of the CuO–ZnO solid solution, respectively.

#### Activity test and copper metal surface area

Figs. 6 and 7 display the reaction temperature dependence of the CO conversion (based on carbon) and the DME yield, respectively. No hydrocarbon byproducts except CO<sub>2</sub> were observed for all the activity tests. The CO conversions and the DME yields over CZA series sharply increased with the rise of the reaction temperature while they smoothly increased over CZAMn series. DME selectivities for all catalysts were relatively constant and were in the range of 63–68% under the applied reaction conditions.

Interestingly, even though all the CZA precursors and the corresponding calcined samples showed similar XRD patterns, each CZA catalyst possessed different activity. The highest catalytic activity was exhibited by CZA–B and CZA–C. The addition of manganese to the Cu–Zn–Al though is believed to increase the copper particles dispersion, does not apparently increase the catalytic activity. It can be seen that at a low reaction temperature (240 °C), CZAMn–A precipitated using Na<sub>2</sub>CO<sub>3</sub> showed higher activity than CZA–A did. This result agrees qualitatively with the results reported in the literature [12]. However, at higher reaction temperatures, the activity of CZAMn–A never surpassed the activity of CZA–B or CZA–C. Meanwhile, the other CZAMn catalysts exhibited the lowest activity.

In spite of some controversies on the active species responsible for controlling the reactivity of Cu–Zn-based catalyst, Nakamura et al. noted that a certain ratio of

**Fig. 6** Variations of CO conversion with reaction temperature over CZA/ $\gamma$ - $\text{Al}_2\text{O}_3$  series and CZAMn/ $\gamma$ - $\text{Al}_2\text{O}_3$  series: (filled square) CZA-A/ $\text{Al}_2\text{O}_3$ , (open square) CZAMn-A/ $\text{Al}_2\text{O}_3$ , (filled triangle) CZA-B/ $\text{Al}_2\text{O}_3$ , (triangle) CZAMn-B/ $\text{Al}_2\text{O}_3$ , (filled circle) CZA-C/ $\text{Al}_2\text{O}_3$ , and (circle) CZAMn-C/ $\text{Al}_2\text{O}_3$

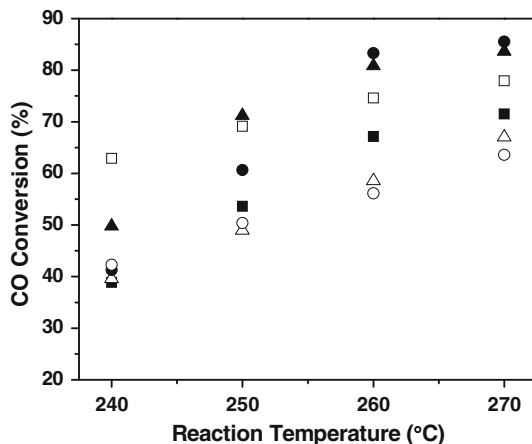
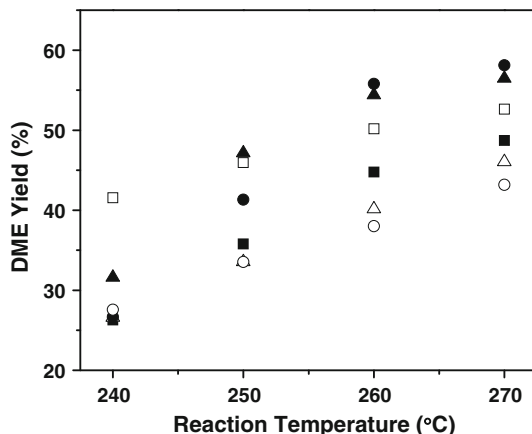


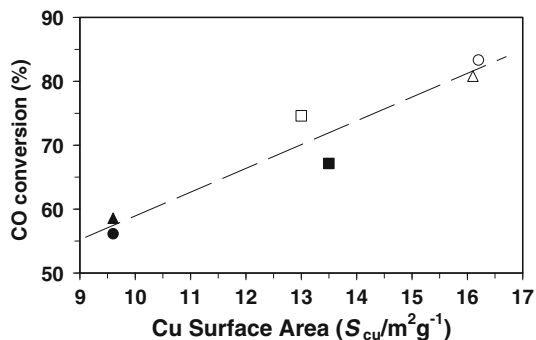
**Fig. 7** Variations of DME yield with reaction temperature over CZA/ $\gamma$ - $\text{Al}_2\text{O}_3$  series and CZAMn/ $\gamma$ - $\text{Al}_2\text{O}_3$  series: (filled square) CZA-A/ $\text{Al}_2\text{O}_3$ , (open square) CZAMn-A/ $\text{Al}_2\text{O}_3$ , (filled triangle) CZA-B/ $\text{Al}_2\text{O}_3$ , (triangle) CZAMn-B/ $\text{Al}_2\text{O}_3$ , (filled circle) CZA-C/ $\text{Al}_2\text{O}_3$ , and (circle) CZAMn-C/ $\text{Al}_2\text{O}_3$



$\text{Cu}^+/\text{Cu}^0$  must exist to control the specific activity [24]. The total copper metal surface area is commonly used to express the number of the active species. The copper surface area ( $S_{\text{Cu}}$ ) of the fresh catalysts, the Cu particle size ( $t_{\text{Cu}}$ ), and the Cu dispersion ( $D_{\text{Cu}}$ ) are given in Table 2. The copper particle size is calculated using the equation of  $t_{\text{Cu}} = 6/(S_{\text{Cu}} \cdot \rho_{\text{Cu}})$ , where  $\rho_{\text{Cu}} = 8.92 \text{ g cm}^{-3}$  is the copper density. The copper dispersion is estimated from  $D_{\text{Cu}} = S_{\text{Cu}}/\text{Cu}_{\text{TPR}} \cdot 100\%$ , where  $\text{Cu}_{\text{TPR}}$  is the total concentration of copper determined from the TPR analysis [25]. Data in Table 2 show that the copper surface area increases with the increase of the copper dispersion and with the decrease of the copper particle size.

In our experiments, a good proportional correlation between the copper metal surface area and the catalytic activity is summarized in Fig. 8. As can be seen from the figure, CZA-B and CZA-C containing the highest copper surface areas show the highest activity. On the contrary, the lowest catalytic activity shown by CZAMn-B and CZAMn-C is in agreement with the lowest copper surface area in both catalysts. Meanwhile, CZA-A and CZAMn-A display moderate activity. These results indicate that coprecipitation using a bicarbonate solution or a carbonate/

**Fig. 8** Correlation of the catalytic activity (in terms of CO conversion) with the copper surface area at 260 °C,  $H_2/CO = 3/2$ , pressure 4.13 MPa, and GHSV = 6000  $h^{-1}$ : (filled square) CZA–A, (open square) CZAMn–A, (filled triangle) CZA–B, (triangle) CZAMn–B, (filled circle) CZA–C, and (circle) CZAMn–C



bicarbonate buffer results in a Cu–Zn–Al catalyst with a greater copper surface area. In contrast, these precipitants are not suitable for the Cu–Zn–Al–Mn preparation. Our experimental results indicate that the activity of our methanol synthesis catalyst is strongly associated with the number of  $Cu^0$  similarly to the findings of other works [3, 7]. This active species is correlated to the total copper surface area. The presence of a greater number of  $Cu^+$  in the CuO–ZnO solid solution probably contributes to the higher activity of CZAMn–A than that of CZA–A. This assumption is on the basis of the TPR analysis of CZAMn–A where it showed the reductions of a minor amount of amorphous CuO and a major amount of CuO–ZnO alloy.

## Conclusions

Cu–Zn–Al-based catalyst for methanol synthesis is a structure sensitive material and its activity is strongly dependent on the preparation method. Our results clearly demonstrate that a Cu–Zn–Al-based catalyst prepared by the coprecipitation technique using an aqueous carbonate solution requires a proper selection of the carbonate source and treatment controls in order to obtain a structurally active Cu–Zn–Al precursor (i.e. a precursor containing HTlc-like layered double hydroxides).

It was found that the most responsible factor in determining the catalytic activity of the Cu–Zn–Al-based catalyst is rather the preparation method than the incorporation of manganese as the structure modifier. There is a substantial correlation between the reactivity of the catalyst and the copper metal surface area. High catalytic reactivity is observed for the catalyst (Cu–Zn–Al or Cu–Zn–Al–Mn) derived from the precursor possessing HTlc-like layered double hydroxides.

## References

1. Prasad PSS, Bae JW, Kang SH, Lee YJ, Jun KW (2008) Fuel Proc Technol 89:1281
2. Sofianos AC, Scurrill MS (1991) Ind Eng Chem Res 30:2372
3. Venugopal A, Palgunadi J, Jung KD, Joo OS, Shin CH (2008) Catal Lett 123:142
4. Klier K (1982) Advance in catalysis. Academic Press, New York, p 243

5. Höppener RH, Doesburg EBM, Scholten JJF (1986) *Appl Catal* 25:109
6. Meshkini F, Taghizadeh M, Bahmani M (2010) *Fuel* 89:170
7. Venugopal A, Palgunadi J, Deog JK, Joo OS, Shin CH (2009) *J Mol Catal A Chem* 302:20
8. Busetto C, Piero GD, Manara G (1984) *J Catal* 85:260
9. Frost RL, Ding Z, Martens WN, Johnson TE (2003) *Thermochim Acta* 398:167
10. Li JL, Inui T (1996) *Appl Catal A Gen* 137:105
11. Fujita S, Kanamori Y, Satriyo AM, Takezawa N (1998) *Catal Today* 45:241
12. Li J, Zhang W, Gao L, Gu P, Sha K, Wan H (1997) *Appl Catal A Gen* 165:411
13. Tan Y, Xie H, Cui H, Han Y, Zhong B (2005) *Catal Today* 104:25
14. Matulewicz ERA, Keijser MS, Mol JC, Kapteijn F (1984) *Thermochim Acta* 72:111
15. Evans JW, Wainwright MS, Bridgewater AJ, Young DJ (1983) *Appl Catal* 7:75
16. Fang D, Liu Z, Meng S, Wang L, Xu L, Wang H (2005) *J Nat Gas Chem* 14:107
17. Stone FS, Waller D (2003) *Top Catal* 22:305
18. Trifirò F, Vaccari A, Del Piero G (1988) *Characterization of porous solids*. Elsevier, Amsterdam
19. Fujita SI, Moribe S, Kanamori Y, Takezawa N (2000) *Reac Kinet Catal Lett* 70:11
20. Robinson WRAM, Mol JC (1990) *Appl Catal* 60:61
21. Qi GX, Zheng XM, Fei JH, Hou ZY (2001) *J Mol Catal A Chem* 176:195
22. Fei JH, Yang MX, Hou ZY, Zheng XM (2004) *Energy Fuels* 18:1584
23. Chen HY, Lin J, Tan KL, Li J (1998) *Appl Surf Sci* 126:323
24. Nakamura J, Uchijima T, Kanai Y, Fujitani T (1996) *Catal Today* 28:223
25. Velu S, Suzuki K, Osaki T (1999) *Catal Lett* 62:159